# **RESEARCH PAPER**

# Green Synthesis of Cobalt Oxide Nanoparticles Using Rosmarinus Officinalis L. Leaf Extract: Characterization and Evaluation of Enzyme Inhibition and Antimalarial Potential

Khilowd Omran Ali <sup>1</sup>, Rana A. K. Al-Refai'a <sup>2\*</sup>, Zainab Shakir Addullah Al-Ali <sup>3</sup>, Saad Abdulmajeed Kareem <sup>4</sup>

- <sup>1</sup> Al-Mussaib Technical College, Al-Furat Al-Awsat Technical University, Iraq
- <sup>2</sup> Department of Chemistry, College of Science, University of Babylon, Iraq
- <sup>3</sup> Department of Chemistry, College of Science, University of Basrah, Iraq
- <sup>4</sup>Research and Development Department, Hilla Textile Factory, The Company for Textile Industries, Iraq

#### ARTICLE INFO

#### Article History:

Received 27 June 2025 Accepted 28 September 2025 Published 01 October 2025

#### Keywords:

Beta-hematin Cobalt oxide nanoparticles Enzyme inhibitors Green synthesis Nanoparticles

#### **ABSTRACT**

The green synthesis of cobalt oxide nanoparticles (Co<sub>3</sub>O<sub>4</sub>-NPs) using Rosmarinus officinalis L. leaf extract offers a sustainable and biocompatible route for nanomaterial production. GC-MS analysis of the aqueous extract identified 24 phytochemicals, including reducing agents (e.g., octadecanal, bicyclo[3.1.1]heptane-3-one) and stabilizers (e.g., cis-vaccenic acid, α-pinene), which facilitated Co<sup>2+</sup> reduction and nanoparticle capping via electron donation and steric hindrance. The synthesized Co<sub>3</sub>O<sub>4</sub>-NPs were characterized by UV-Vis, FT-IR, SEM, EDX, and XRD, revealing a crystalline monoclinic structure (30-54 nm) with high purity. The nanoparticles exhibited dose-dependent acetylcholinesterase (AChE) inhibition (70% at 1000 µg/mL), attributed to their interaction with the enzyme's active site. Notably, Co<sub>3</sub>O<sub>4</sub>-NPs suppressed beta-hematin formation by 80% at 50 µg/mL, outperforming chloroquine, likely due to heme-binding surface properties. This dual functionality—enzyme inhibition and antimalarial activity—positions R. officinalis-derived Co<sub>3</sub>O<sub>4</sub>-NPs as promising candidates for neurodegenerative and antiparasitic therapies.

#### How to cite this article

Omran Ali K., Al-Refai'a R., Addullah Al-Ali Z., Kareem S. Green Synthesis of Cobalt Oxide Nanoparticles Using Rosmarinus officinalis L. Leaf Extract: Characterization and Evaluation of Enzyme Inhibition and Antimalarial Potential. J Nanostruct, 2025; 15(4):2100-2111. DOI: 10.22052/JNS.2025.04.050

#### INTRODUCTION

Nanoparticles (NPs) are one of the most promising sectors, with diverse applications, particularly in biomedical applications. Their use as a link between bulk substances and atom or molecular structures exhibit distinct features according to their unique properties [1,2]. They are extremely small materials ranging in size from 1 to 100 nanometres [3]. Today, nanoparticles

\* Corresponding Author Email: sci.rana.abdul@uobabylon.edu.iq

are important components of many applications in consumer products, medicine, chemicals, environmental science, energy, agriculture, and even communication [4]. Currently, there is a growing interest of researchers as regards cobalt oxide nanoparticles and their application in biomedicine. Nanoparticles have, however, revolutionised medicine by enabling new methods of disease diagnosis and treatment [5].

The enzyme inhibitory properties of cobalt oxide nanoparticles ( ${\rm Co_3O_4}$  NPs) stem from their distinctive characteristics and biomolecule binding capabilities [6]. Research on enzyme inhibition enables scientists to understand disease processes while discovering new therapeutic targets. The development of new enzyme inhibitors for different diseases can be achieved through the use of  ${\rm Co_3O_4}$ -NPs [7].

The semi-conductivity, piezoelectricity and distinctive optical properties of Co3O4 NPs make them a promising "smart weapon" against drug-resistant microbes. The toxicity profile of these nanoparticles indicates they could replace traditional antibiotics as an alternative treatment. [8]. The study of cobalt oxide nanoparticle-based nanomaterials continues for various applications including nanosensors, energy storage, cosmetics, nanoelectronic devices, and nano-optical devices [9]. Even though it is a material with great potential, very few studies have assessed CO<sub>3</sub>O<sub>4</sub> nanoparticles for various biological applications due to the numerous reports of their possible harmful effects [10].

The formation of nanoparticles utilizing plants as a precursor has received much more attention in the last ten years. As an alternative to standard chemical and physical approaches, the green synthesis of nanoparticles using plants offers an economical, resilient, eco-friendly, and easily accessible process [11,12]. Several plant secondary metabolites are bioactive molecules that can be used to treat a variety of ailments, such as reducing damage caused by reactive oxygen species, which have been linked to many human health issues, including arthritis, cancer, inflammatory illnesses, and heart disease [13].

Alzheimer's disease (AD) is a progressive neurological sickness that is still not fully understood; it has been reported that over 50 million people worldwide are affected by it [14].

Nonetheless, several drugs approved for treating Alzheimer's disease symptoms have been linked to hepatotoxicity, an increased risk of urinary incontinence, and an increased risk of bradycardia, among other cardiovascular side effects. Individualised combination therapy may need to be adjusted based on disease stage and may be personalised to each patient. [15,16]. Because of its critical function in the breakdown of the neurotransmitter acetylcholine, acetylcholinesterase (AChE) is an attractive target

for developing mechanism-based inhibitors. The search for new medications continues to concentrate on those that can enter the brain efficiently, have fewer side effects, and have a high bioavailability [14].

AChE inhibitors, like galantamine is currently thought to be the best therapy for the cognitive symptoms of Alzheimer's disease (AD), nevertheless, gastrointestinal problems may result from these drugs [17].

Malaria is another common global disease, particularly in developing countries. Malaria parasites cause hemoglobin breakdown within the host's red blood cells, allowing them to use the resultant amino acids for protein synthesis during their proliferation, which is necessary for survival [18]. Metallic nanoparticles (MNPs), a form of nanoparticle, have made major contributions to malaria treatment, especially during the human infection phase and in affecting the mosquito vector. According to comprehensive reviews by Rahman et al. [19] and Veeragoni et al. [20], Rana et al. [4] the common MNPs considered for these applications are silver, gold, palladium and copper.

The current study aims to develop a simple and environmentally friendly approach for the manufacture of nanosized  ${\rm CO_3O_4}$  using plant extract as a reducing and capping agent. The surface qualities, size, shape, and crystallographic structure of  ${\rm CO_3O_4}$  nanoparticles are examined and addressed, as well as their potential applications as enzyme and beta-hematic or hemozion inhibitor.

### **MATERIALS AND METHODS**

Materials and Instrumentation

The research work took place in the chemistry laboratory located at the University of Babylon in Iraq. The Sigma-Aldrich company supplied all chemicals and reagents while the local market provided rosemary leaves. The present study utilized multiple equipment including a UV-Vis double beam spectrophotometer, FTIR, XRD, Scanning Electron Microscope (SEM) and EDX spectroscopy.

### The extraction of plant meterial

Rosemary leaves (Rosmarinus Officinalis L.) were provided from Iraqi local market, after getting 20 g were washed two times with distilled- water and once with a solution of 5% ethanol to completely eradicate possible microbial contaminations on the leaf surface. After that, the leaves dried out

after being in an oven at 80 °C for a day. The dried leaves were ground into a fine powder.

The aqueous extract was finally produced by boiling 100 mL of distilled water with the powdered leaves for one hour under continuous stirring at 600 rpm. After heating, the sample was kept for extra 24 h in order to eliminate any residual contaminants, the resultant plant extract was stored for some future use [21].

#### Green Synthesis of Cobalt Oxide Nanoparticles

The synthesis was flowed the published work [22] with some modification. Briefly, plant extract (30 mL) was heated at 85°C with 0.2 M cobalt chloride hexahydrate (CoCl<sub>2</sub>. 6H<sub>2</sub>O) with continuous stirring at 600 rpm for 30 minutes then sodium hydroxide (pH 14) was added for extra thirty minutes till a change in colour of the resultant solution from pink to dark grey was detected, and then centrifuged at 10000 rpm for 10 min. Finally, the precipitates were dried at 500°C for 2 hours, grinded and subjected for characterization.

#### Nanoparticle Characterizations

The crystalline structure of CO<sub>2</sub>O<sub>4</sub>-NPs was estimated from XRD (PANalytical factory default; radiation = Cu Kα (1.5405 Å); working condition = 30 kV and 8 mA) analysis. The nano-sized surface structural modification and their elemental compositions were analysed from SEM and EDX spectroscopy, all three measurements were determined at Alkhora Lab for Scientific Research Iraq- Baghdad. The UV-Visible spectrophotometer was model UV-1700 double-beam from Shimadzu (Japan) was used to identify the photosensitive and optical properties of this nanoparticle. The formation and association functional group of nanoparticles were observed by FT-IR spectroscopy 380 spectra Bruker from (Germany) with a wavelength limiting 4000 cm<sup>-1</sup> to 400 cm<sup>-1</sup>.

# Acetylcholinesterase inhibitory assay

The enzyme (AChE) inhibition activity was determined using the spectrophotometric method as refer to published procedure [23]. The experimental protocol and testing conditions were followed.two-fold dilutions of  ${\rm CO_3O_4}$ -NPs (1,000, 500, 250, 125, and 62.5 µg/mL) was employed. The substrate acetyl choline iodide (AChI) was used to test AChE inhibitory action. Solution A (0.0002 M) in 0.062 M sodium phosphate buffer (pH 8, 880 µL) was combined with solution B, the test sample (40

 $\mu$ L), and either acetyl cholinesterase solution (40  $\mu$ L) along with incubation at 25°C for 15 minutes. The reaction started when (40  $\mu$ L) Ach was added

then, the hydrolysis was detected at 412 nm. The concentrations of the analyzed compounds that inhibit the hydrolysis of the ACh-substrate were investigated by assessing the effect of increasing concentration of the compound on the inhibition values.

#### Beta-hematin formation

Freshly stock solution of heme was prepared by dissolving 0.0163 g of hemin chloride in 0.2 MNaOH. The initial solution was centrifuged at 7 g for 15 minutes to eliminate any remaining hematin crystals. The concentration was 58,400 mM in 0.1 M NaOH, as determined at 385 nm using the UV-Vis double-beam spectrophotometer, which was employed to record all absorption spectra. The synthesis of beta-hematin (BH) corresponds to the specified method [4]. Hemin chloride (10 mL) was heated in an acetate buffer (0.56 M, pH 5) at 70°C without CQ or CO<sub>3</sub>O<sub>4</sub>-NPs, while varying CQ concentrations (10-50 µM) and CO<sub>3</sub>O<sub>4</sub>-NPs concentrations (10-50 µg/mL) individually. One mL of heme solution was extracted at specified intervals, and BH formation was assessed. The absorbance of each sample was measured at 400 and 700 nm following the separate heating of treated and untreated heme solutions to confirm BH production. As a result, heme fractions were determined after being converted to BH using the following Eq. (1) [24].

Fractions = 
$$\frac{(A_{400} - A_{700})control - (A_{400} - A_{700})Sample}{(A_{400} - A_{700})control}$$
(1)

#### **RESULTS AND DISCUSSION**

GC-MS Analysis of Aqueous Extract of Rosmarinus Officinalis L L. for Cobalt Oxide Nanoparticles  $(Co_3O_4 \text{ NPs})$  Synthesis

The aqueous extract of *Rosmarinus Officinalis* L. was analyzed using GC-MS (Fig. 1) to identify phytochemicals that could play a role in the green synthesis of cobalt oxide nanoparticles ( $Co_3O_4$  NPs). The analysis revealed 24 compounds, dominated by fatty acids (e.g., cis-vaccenic acid, trans-13-octadecenoic acid), terpenes (e.g.,  $\alpha$ -pinene), and phenolic derivatives (e.g., 2-methoxy-4-vinylphenol). Notably, the extract contained long-chain alkanes and fatty acid derivatives, which are crucial for nanoparticle

J Nanostruct 15(4): 2100-2111, Autumn 2025



stabilization, while antioxidants like carnosic acid and rosmarinic acid were absent, as they typically require LC-MS detection.

(Table1) lists key compounds aqueous extract of Rosmarinus Officinalis L. with their structures and their roles in  $Co_3O_4$  NPs synthesis. The identified

Reference							
2 4.38 0.06 Octadecanal CultuO; 288.49	No.	time in	Peak			weight	Structure
3 6.58 0.10 Cis-vacceric acid CuHuO, 282.26	1	3.80	0.04	2-Eicosanol	C <sub>20</sub> H <sub>42</sub> O	298.56	ОН 
4 7.19 0.05   Bicycle[3.1.1]hept-2-ene (Ajpha-pirene)   C.Hu   94.16	2	4.38	0.06	Octadecanal	C <sub>18</sub> H <sub>36</sub> O <sub>2</sub>	268.49	(^\\\\\\\\\\\\\\\\\\\\\\\\\\\\\\\\\\\\
4       7.19       0.05       (Alpha-pinene)       C.H <sub>10</sub> 94.16       94.16         5       7.90       0.33       Bicyclo(3.1.1]heptane-3-one       C.H <sub>10</sub> 110.16       □         6       8.39       0.34       4-Methyldocosane       C <sub>22</sub> H <sub>10</sub> 324.46       □         7       8.60       0.17       Cyclopropaneundecanal       C <sub>42</sub> H <sub>10</sub> O       210.36       □         8       8.82       0.40       2-Methoxy-4-vinylphenol       C <sub>41</sub> H <sub>10</sub> O       150.18       □         9       9.56       0.21       1-Heptadecene       C <sub>12</sub> H <sub>10</sub> O       314.47       □         10       9.81       0.52       Oxalic acid, dodecyl sobutyl ester       C <sub>12</sub> H <sub>10</sub> O       314.47       □         11       9.87       0.78       2,1,3-Benthiladazole       C <sub>14</sub> H <sub>10</sub> O       122.17       □         12       10.03       0.41       Benzeneethanol       C <sub>14</sub> H <sub>10</sub> O       122.17       □         13       10.44       0.38       Octadecosine       C <sub>14</sub> H <sub>10</sub> O       318.58       HO         14       10.91       0.53       Diethyl phthalate       C <sub>14</sub> H <sub>10</sub> O       222.24       □         15       11.34       0.47       1.	3	6.58	0.10	Cis-vaccenic acid	C <sub>18</sub> H <sub>34</sub> O <sub>2</sub>	282.26	О О О О О О О О О О О О О О О О О О О
5       7,90       0.33       Bicyclo(3.1.1)heptane-3-one       C <sub>H</sub> H <sub>sQ</sub> 110.16         6       8.39       0.34       4-Methyldocosane       C <sub>H</sub> H <sub>sQ</sub> 324.46         7       8.60       0.17       Cyclopropaneundecanal       C <sub>H</sub> H <sub>sQ</sub> O       210.36         8       8.82       0.40       2-Methosy-4-vinylphenol       C <sub>H</sub> H <sub>sQ</sub> O       150.18         9       9.66       0.21       1-Heptadecene       C <sub>H</sub> H <sub>sQ</sub> O       150.18         10       9.81       0.52       Oxalic acid, dodecyl toolutyl ester       C <sub>H</sub> H <sub>sQ</sub> O       314.47         11       9.87       0.78       2.1, 3-Benthladiazole       C <sub>H</sub> H <sub>sQ</sub> O       122.17         12       10.03       0.41       Benzeneethanol       C <sub>H</sub> H <sub>sQ</sub> O       122.17         13       10.44       0.38       Octadecosane       C <sub>H</sub> H <sub>sQ</sub> O       122.17         14       10.91       0.26       1-Henelcosanol       C <sub>H</sub> H <sub>sQ</sub> O       318.58       HO         15       11.19       0.53       Diethyl phthalate       C <sub>H</sub> H <sub>sQ</sub> O       222.24       Image: Company of the methyl-12-tetradecen-1-coloridate       C <sub>H</sub> H <sub>sQ</sub> O       222.47       Image: Company of the methyl-12-tetradecen-1-coloridate       C <sub>H</sub> H <sub>sQ</sub> O       222.47       Image: Coloridat	4	7.19	0.05		C <sub>7</sub> H <sub>10</sub>	94.16	
7       8.60       0.17       Cyclopropaneundecanal       C <sub>ti</sub> H <sub>tis</sub> O       210.36       □         8       8.82       0.40       2-Methoxy-4-virylphenol       C <sub>ti</sub> H <sub>tis</sub> O₁       150.18       □         9       9.66       0.21       1-Heptadecene       C <sub>ti</sub> H <sub>tis</sub> O₁       314.47       □         10       9.81       0.52       Oxalic acid, dodecyl isobutyl ester       C <sub>ti</sub> H <sub>tis</sub> O₂       314.47       □         11       9.87       0.78       2,1,3-Benzthiadiazole       C <sub>ti</sub> H <sub>tis</sub> O₂       314.47       □         12       10.03       0.41       Benzeneethanol       C <sub>ti</sub> H <sub>tis</sub> O₂       122.17       □         13       10.44       0.38       Octadecosane       C <sub>ti</sub> H <sub>tis</sub> O₂       122.17       □         14       10.91       0.26       1-Heneicosanol       C <sub>ti</sub> H <sub>tis</sub> O₂       318.58       HO         15       11.19       0.53       Diethyl phthalate       C <sub>ti</sub> H <sub>tis</sub> O₂       222.24       □         16       11.34       0.47       11.75-methyl-12-tetradecen-1- c <sub>ti</sub> C <sub>ti</sub> H <sub>tis</sub> O₂       228.47       □         17       11.53       0.31       1-Nonadecene       C <sub>ti</sub> H <sub>tis</sub> O₂       228.47       □         18       11.62	5	7.90	0.33	Bicyclo[3.1.1]heptane-3-one	C <sub>7</sub> H <sub>10</sub> O	110.16	O
8 8.82 0.40 2-Methoxy-4-vinylphenol C <sub>1</sub> H <sub>14</sub> O <sub>2</sub> 150.18 HO 9 9.66 0.21 1-Heptadecene C <sub>1</sub> H <sub>24</sub> 238.46 10 9.81 0.52 Oxalic acid, dodecyl isobutyl ester C <sub>2</sub> H <sub>34</sub> O <sub>4</sub> 314.47 11 9.87 0.78 2, 1, 3-Benzthiadiazole C <sub>4</sub> H <sub>3</sub> N.5 136.17 12 10.03 0.41 Benzeneethanol C <sub>4</sub> H <sub>3</sub> O 122.17 13 10.44 0.38 Octadecosane C <sub>2</sub> H <sub>3</sub> O 318.58 HO 14 10.91 0.26 1-Henecosanol C <sub>1</sub> H <sub>4</sub> O 318.58 HO 15 11.19 0.53 Diethyl phthalate C <sub>2</sub> H <sub>3</sub> O 222.24 16 11.34 0.47 11.13-Dimethyl-12-tetradecen-1- C <sub>2</sub> H <sub>3</sub> O 222.24 17 11.53 0.31 1-Nonadecene C <sub>3</sub> H <sub>3</sub> O 220.36 Ho methyl-duct-zenyl-6- methyl-duct-zenyl-6- methyl-buct-zenyl-6- meth	6	8.39	0.34	4-Methyldocosane	C <sub>23</sub> H <sub>48</sub>	324.46	\\\\\\\\\\\\\\\\\\\\\\\\\\\\\\\\\\\\\\
8 8.82 0.40 2-Methoxy-4-winylphenol C <sub>3</sub> H <sub>10</sub> O <sub>2</sub> 150.18	7	8.60	0.17	Cyclopropaneundecanal	C <sub>14</sub> H <sub>26</sub> O	210.36	Δο
10 9.81 0.52 Oxalic acid, dodecyl isobutyl ester CuHusO4 314.47  11 9.87 0.78 2, 1, 3-Benzthiadiazole CμHusO5 136.17  12 10.03 0.41 Benzeneethanol CaHusO 122.17  13 10.44 0.38 Octadecosane CaHus 394.77	8	8.82	0.40	2-Methoxy-4-vinylphenol	$C_9H_{10}O_2$	150.18	HO
11 9.87 0.78 2, 1, 3-Benzthiadiazole C <sub>4</sub> H <sub>18</sub> D 136.17	9	9.66	0.21	1-Heptadecene	C <sub>17</sub> H <sub>34</sub>	238.46	<b>////////</b>
12 10.03 0.41 Benzeneethanol C <sub>4</sub> H <sub>19</sub> O 122.17	10	9.81	0.52	Oxalic acid, dodecyl isobutyl ester	C <sub>18</sub> H <sub>34</sub> O <sub>4</sub>	314.47	~~~~~~~~~~~~~~~~~~~~~~~~~~~~~~~~~~~~~~
13 10.44 0.38 Octadecosane C <sub>23</sub> H <sub>36</sub> 394.77	11	9.87	0.78	2, 1, 3-Benzthiadiazole	$C_6H_4N_2S$	136.17	N <sub>N</sub> S
14 10.91 0.26 1- Heneicosanol C <sub>21</sub> H <sub>44</sub> O 318.58 HO 1.1.19 0.53 Diethyl phthalate C <sub>11</sub> H <sub>14</sub> O <sub>4</sub> 222.24	12	10.03	0.41	Benzeneethanol	C <sub>8</sub> H <sub>10</sub> O	122.17	Он
11.19	13	10.44	0.38	Octadecosane	C <sub>28</sub> H <sub>58</sub>	394.77	^^^
11.34 0.47 11.13-Dimethyl-12-tetradecen-1- ol acetate  17 11.53 0.31 1-Nonadecene C18H18 266.51  18 11.62 0.51 1-Formyl-2,2-dimethyl-3-trane-(3-methyl-but-2-enyl)-6- methylidene-cyclohexane  19 11.82 0.58 22-Tricosenoic acid C18H180 352.60  20 12.37 0.37 Trans-13-octadeceenoic acid C18H180 282.47  21 12.47 0.60 Octadecane C18H18 254.50  22 12.63 0.42 5-Methyl-2-5-docosene C21H18 322.62  23 12.89 0.47 1-Nonadecene C18H18 266.51	14	10.91	0.26	1- Heneicosanol	C <sub>21</sub> H <sub>44</sub> O	318.58	но
11.54 0.47 ol acetate CisHisi 266.51  17 11.53 0.31 1-Nonadecene CisHisi 266.51  18 11.62 0.51	15	11.19	0.53	Diethyl phthalate	C12H14O4	222.24	
18	16	11.34	0.47		C18H34O2	282.47	ļ
18     11.62     0.51     methyl-but-2-enyl)-6-methylidene-cyclohexane     C18H2AO     220.36       19     11.82     0.58     22-Tricosenoic acid     C23H4AO2     352.60       20     12.37     0.37     Trans-13-octadeceenoic acid     C18H2AO2     282.47       21     12.47     0.60     Octadecane     C18H3B     254.50       22     12.63     0.42     5-Methyl-2-5-docosene     C23H46     322.62       23     12.89     0.47     1-Nonadecene     C18H3B     266.51       24     13.23     0.38     1,4-Benzenediol, bis(1,1-dimethylethyl)-dimethylethyly-dimethylethyl)-dimethylethyly-dimethyly-dimethyly-dimethyly-dimethylethyly-dimethylethyly-dimethyly-dimethyly-dimethyly-dimethyly-dimeth	17	11.53	0.31	1-Nonadecene	C19H38	266.51	<b>*****</b>
20 12.37 0.37 Trans-13-octadeceenoic acid C <sub>18</sub> H <sub>18</sub> O <sub>2</sub> 282.47 O <sub>0H</sub> 21 12.47 0.60 Octadecane C <sub>18</sub> H <sub>18</sub> 254.50  22 12.63 0.42 5-Methyl-z-5-docosene C <sub>28</sub> H <sub>46</sub> 322.62  23 12.89 0.47 1-Nonadecene C <sub>18</sub> H <sub>38</sub> 266.51  24 13.23 0.38 1 <sub>.4</sub> -Benzenediol, bis(1,1-dimethylethyl)- C <sub>28</sub> H <sub>46</sub> F <sub>3</sub> O <sub>2</sub> 472.63	18	11.62	0.51	methyl-but-2-enyl)-6-	C15H24O	220.36	
21 12.47 0.60 Octadecane C <sub>18</sub> H <sub>18</sub> 254.50	19	11.82	0.58	22-Tricosenoic acid	C23H44O2	352.60	<b>&gt;&gt;&gt;&gt;&gt;&gt;</b>
22 12.63 0.42 5-Methyl-2-5-docosene C <sub>23</sub> H <sub>46</sub> 322.62  23 12.89 0.47 1-Nonadecene C <sub>13</sub> H <sub>38</sub> 266.51  24 13.23 0.38 1,4-Benzenediol, bis(1,1-dimethylethyl)-dimethylethyl)-dimethylethyl)-	20	12.37	0.37	Trans-13-octadeceenoic acid	C <sub>18</sub> H <sub>34</sub> O <sub>2</sub>	282.47	~~~~ рон
23 12.89 0.47 1-Nonadecene C <sub>19</sub> H <sub>38</sub> 266.51 OH	21	12.47	0.60	Octadecane	C <sub>18</sub> H <sub>38</sub>	254.50	<b>^</b>
24 13.23 0.38 1,4-Benzenediol, bis(1,1- dimethylethyl)- C <sub>22</sub> H <sub>40</sub> F <sub>5</sub> O <sub>2</sub> 472.63	22	12.63	0.42	5-Methyl-z-5-docosene	C <sub>23</sub> H <sub>46</sub>	322.62	~~
24 13.23 0.38 1,4-Benzenediol, bis(1,1- dimethylethyl)-	23	12.89	0.47	1-Nonadecene	C <sub>19</sub> H <sub>38</sub>	266.51	<b>/////////////////////////////////////</b>
	24	13.23	0.38		$C_{25}H_{45}F_5O_2$	472.63	

compounds can be categorized based on their functions in nanoparticle synthesis. Reducing agents: octadecanal (Peak 2), bicyclo[3.1.1] heptane-3-one (Peak 5), benzeneethanol (Peak 12): These compounds, with aldehyde, ketone, and alcohol groups, donate electrons to reduce  $Co^{2+}$  ions to zerovalent cobalt ( $Co^{0}$ ). Stabilizers and capping agents: fatty acids (cis-vaccenic acid, 22-tricosenoic acid) and alkenes (1-heptadecene, 1-nonadecene): form protective layers around nanoparticles via hydrophobic interactions. Longchain alkanes (octadecane, 4-methyldocosane) and terpenes ( $\alpha$ -pinene): prevent aggregation

by acting as capping agents. Antioxidants and nucleation modulators: 2-methoxy-4-vinylphenol (Peak 8) and 1, 4-benzenediol derivative (Peak 24): enhance stability by scavenging free radicals and controlling nucleation rates.

Proposed Mechanism for Green Synthesis of Co₃O₄ NPs Using Rosmarinus Officinalis L. Aqueous Extract

The green synthesis of cobalt oxide nanoparticles (Co₃O₄ NPs) using *Rosmarinus Officinalis* L. extract proceeds via a three-step mechanism involving reduction, nucleation, and stabilization, mediated

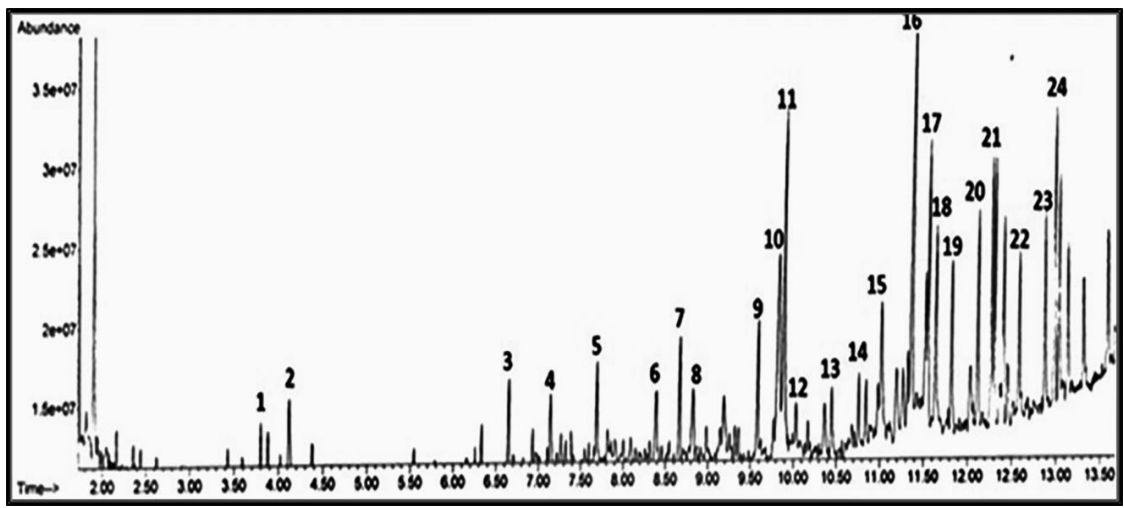


Fig. 1. GC-MS chromatogram of aqueous extract of Rosmarinus Officinalis L.

# 

Fig. 2. The schematic representation suggested mechanism for the green synthesis of Co₃O₄ NPs using aqueous extract of *Rosmarinus Officinalis* L.

by phytochemicals identified in the GC-MS analysis (Fig. 2).

#### 1. Reduction of Cobalt Ions

Key Phytochemicals: Aldehydes (e.g., Octadecanal), ketones (e.g., Bicyclo[3.1.1]heptane-3-one), and alcohols (e.g., Benzeneethanol). Functional groups (–CHO, >C=O, –OH) donate electrons to Co<sup>2+</sup>/Co<sup>3+</sup> ions, reducing them to zerovalent cobalt (Co<sup>0</sup>). Phenolic compounds (e.g., 2-Methoxy-4-vinylphenol) further assist by acting as electron donors and antioxidants.

#### 2. Nucleation and Oxidation

Key Phytochemicals: Terpenes ( $\alpha$ -Pinene), phenolics, and fatty acids. Zerovalent cobalt ( $Co^{\circ}$ ) reacts with dissolved oxygen ( $O_2$ ) or hydroxyl ions ( $OH^{-}$ ) in the aqueous medium, forming cobalt oxide nuclei ( $Co_3O_4$ ): Nucleation is modulated by phytochemicals (e.g.,  $\alpha$ -Pinene), which control the release of  $Co^{\circ}$ , preventing rapid aggregation.

#### 3. Stabilization and Capping

Key Phytochemicals: Fatty acids (Cis-vaccenic acid, 22-Tricosenoic acid), long-chain alkanes (Octadecane), and alkenes (1-Nonadecene). Hydrophobic tails of fatty acids and alkanes surround  $\text{Co}_3\text{O}_4$  NPs, while polar groups (–COOH, –OH) face outward, forming a steric barrier.

#### **UV-Visible Spectrophotometric Analysis**

The first sign that  ${\rm Co_3O_4}$  -NPs were being synthesised was a colour shift in the reaction mixture from yellowish brown to dark grey in thirty minutes at 37 °C. The response mechanism

between components of plant leaf extract and metal ions was investigated using UV–visible spectra.  ${\rm CO_3O_4}$  nanoparticles were liquefied with deionized water and sonicated for extra five min at 30 °C . Then, the absorbance maxima were ascertained for both the nanoparticle solution and the plant extract individually, revealing a broad peak at 300 nm in the plant leaf extract and at 450-510 nm in the green generated  ${\rm Co_3O_4}$ -NPs, as illustrated in (Fig. 2), thereby confirming the production of the nanoparticles (Fig. 3).

# Fourier Transform Infrared (FT-IR)

The FT-IR analysis revealed various functional groups in the plant extract and  $Co_3O_4$  nanoparticles.

A medium peak was noticed at 3549.14, 3473.91 and clear once at 3412.19 cm<sup>-1</sup> corresponding to -OH of alcohol or phenol stretching vibration, carboxylic acid -OH stretch and N-H stretching of amine respectively. The aromatic and unsaturated hydrocarbons' C-H (=C-H stretch) is represented by the plant extracts broad peak at 2931.90 cm<sup>-1</sup>. A sharp peak was noticeable at 1512.24 cm<sup>-1</sup> representing NH<sub>2</sub> in amino acids (NH<sub>3</sub> deformation). The strong peak at 1587.47-1608.69 cm<sup>-1</sup> is characterized by -NH stretch of primary amines. Moreover, one peak presented at 1423.51 cm<sup>-1</sup> can be assigned to -CH<sub>3</sub>. Two sharp peaks were noticed at 1257.63 and 1072.46 cm<sup>-1</sup>, which represent-C-N stretching vibration. C-N-C, N-C=O, and O-C=O bends were all observed at

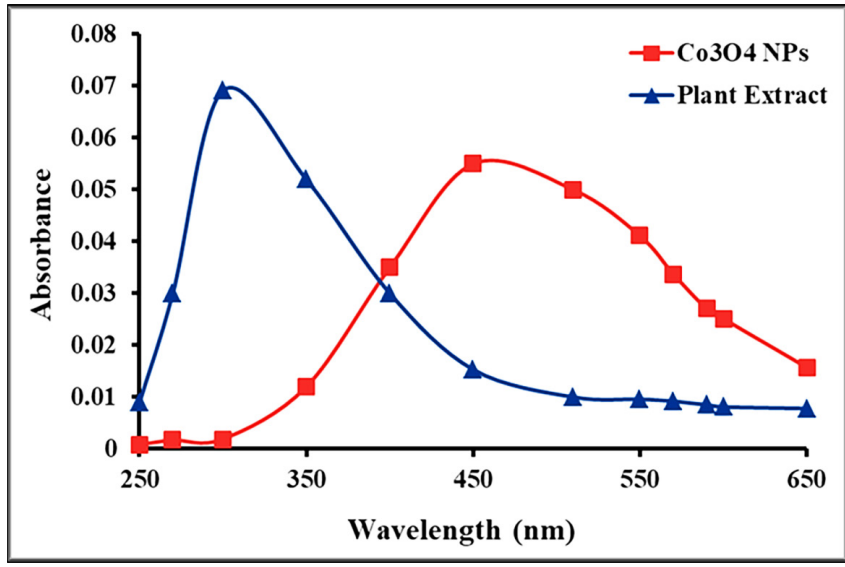


Fig. 3. UV-spectra of the cobalt oxide nanoparticles and rosemary extract.

600-650 cm<sup>-1</sup>, which is the peak of O-C=O bending in carboxylic acids (Fig. 4A).

On the other hand, the obtained FT-IR data of Co<sub>3</sub>O<sub>4</sub>—NPs (Fig. 5B) revealed various absorption peaks, given the various functional group of phytochemicals. The absorption peaks at 3581. 93, 3520.21, 3294.53,3201. 94cm<sup>-1</sup> were assigned the O-H stretch of phenolic compounds, N-H stretch of primary amides, H-C=O: stretch of aldehydes. The aromatic and unsaturated hydrocarbons' C-H (=C-H stretch) is represented at 2937.68 cm<sup>-1</sup>.two peaks were presented at 1658.84 and 1570.11 cm<sup>-1</sup> indicating amide N-H and C=O stretch as a bending vibration of carbonyl groups of flavonoids

and tannins respectively.

Strong peaks at about 1489.10 and 1402.30 cm<sup>-1</sup> as a possible C=O stretch. A medium peak was observed at 1031.95 cm<sup>-1</sup> indicating C-N stretching vibration. Finally, two clear peaks were obtained at 690.54 and 559.38 cm<sup>-1</sup> could be stretching vibration of Co3O4-NPs in the monoclinic structure (Fig. 4B). These peaks suggest the presence of various phytochemicals and functional groups in both the plant extract and Co<sub>3</sub>O<sub>4</sub> nanoparticles.

### Scanning Electron Microscopy (SEM)

(Fig. 5) presents the surface morphology of Co<sub>2</sub>O<sub>4</sub> NPs by SEM (Enclosed and preserving

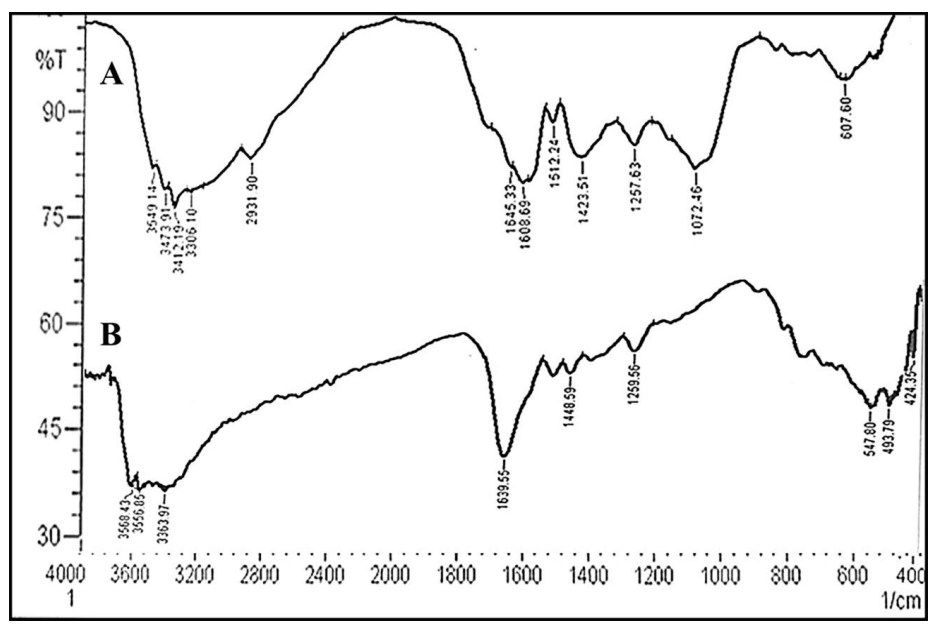


Fig. 4. FT-IR spectra of A. rosemary leaf extract and B. Co<sub>3</sub>O<sub>4</sub>- NPS detected form infrared red spectroscopy.

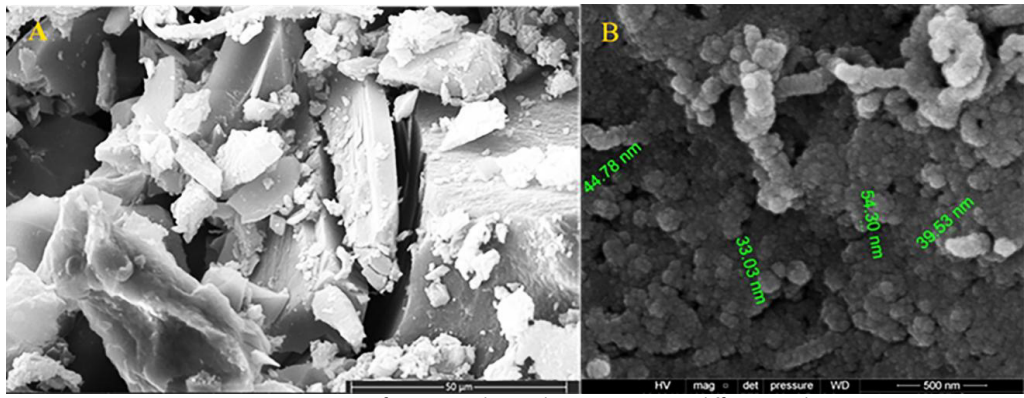


Fig. 5. SEM images of green synthesised Co<sub>3</sub>O<sub>4</sub>-NPs using different scale.

the stability of individual particles are indicated due to the bioactive chemicals resulting in larger particles from the reactivity and attraction of the functional groups. At several scales, were observed by SEM images of Co<sub>3</sub>O<sub>4</sub> nanoparticles which distinctly exhibit nanoparticle-like forms with size distributions between 33 and 54 nm. The generated nanoparticles have quite perfect surfaces.

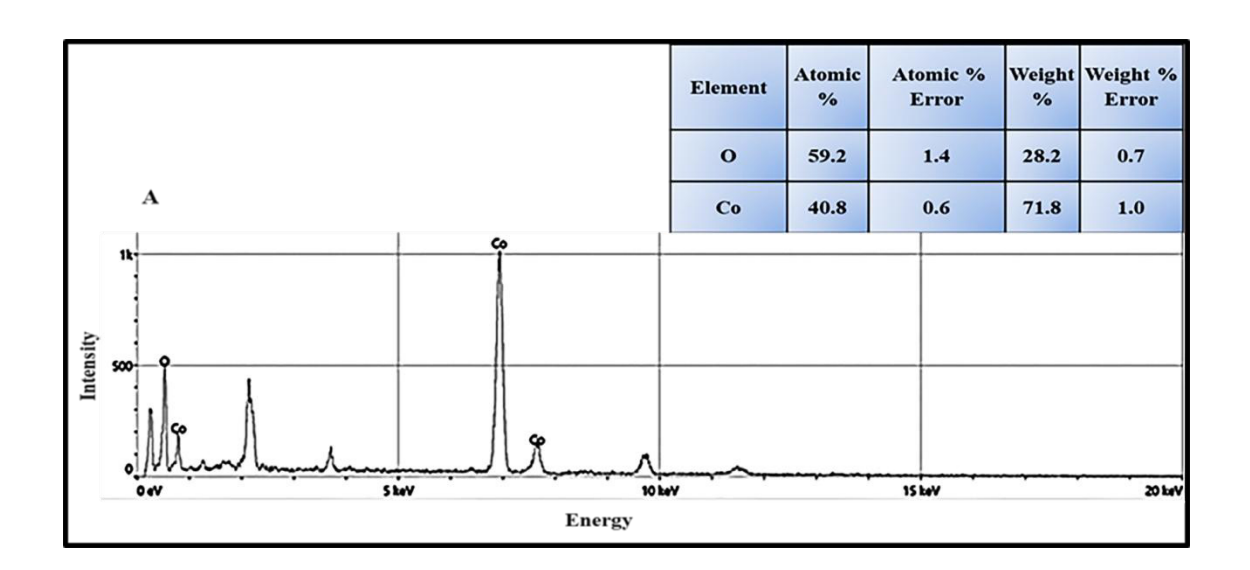
#### Energy Dispersive X-ray Analysis (EDX)

The elemental conformation of the synthesized  ${\rm Co_3O_4}$ -NPs was estimated from EDX analysis at acceleration voltage of 30 kV. EDX analysis confirmed the elemental composition of  ${\rm Co_3O_4}$  nanoparticles, showing major peaks for cobalt (Co) and oxygen (O), with minor carbon peaks from

the plant extract. The elemental composition was 40.8% Cobalt (Co) and 59.2% Oxygen (O), these values match theoretical calculations, indicating good compositional homogeneity as presented in (Fig. 6).

#### XRD Analysis

XRD analysis has confirmed the structural features and crystalline character of green-produced  ${\rm Co_3O_4}$ -NPs. The XRD pattern of  ${\rm Co_3O_4}$ -NPs obtained from rosemary leaf extract is shown in (Fig. 7). As shown in this Figure, the intensity peaks at 32.25°, 36.59°, 39.24°, 45.26°, 59.42°, and 67.35° correspond to the planes at 220, 311, 222, 400, 511, and 440, respectively. This finding is in strong correspondence with previous studies [25,26].



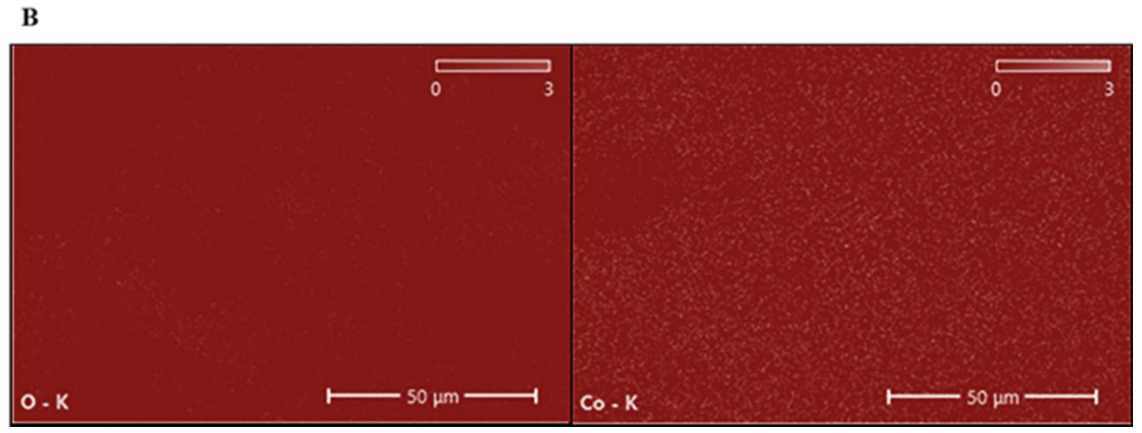


Fig. 6. A. EDX spectrum, B. the counts map of green synthesised  $Co_3O_4$ -NPs.

#### Enzyme inhibitor

Anti-cholinesterase compounds have demonstrated effectiveness in alleviating the symptoms associated with Alzheimer's disease. These compounds inhibit the enzyme that facilitates the breakdown of acetylcholine, thereby increasing its levels and mitigating the related symptoms [27,28].

In this work the ability of green synthesised  ${\rm Co_3O_4\text{-}NPs}$  as anticholinesterase has been explored. (Fig. 8) represents the potential enzyme inhibitory of green synthesized  ${\rm Co_3O_4\text{-}NPs.}$  The

results show the possible enzyme inhibition of green- produced  ${\rm Co_3O_4}$ -NPs, these nanoparticles demonstrated good acetylcholinesterase (AChE) inhibitory activity at 1,000 µg/mL. The highest effectiveness noted for these NPs against AChE was 77%, next, 68, 59, 54, and 49% at 500, 250, 125, and 62.5 µg/mL, respectively, as shown in (Fig. 8). For the control galantamine the maximum activity observed was 80% at 1000 µg/mL followed by 74, 68, 56 and 58% at 500, 250, 125, and 62.5 µg/mL, respectively.

The inhibitory activity of Co<sub>3</sub>O<sub>4</sub>- NPs may be

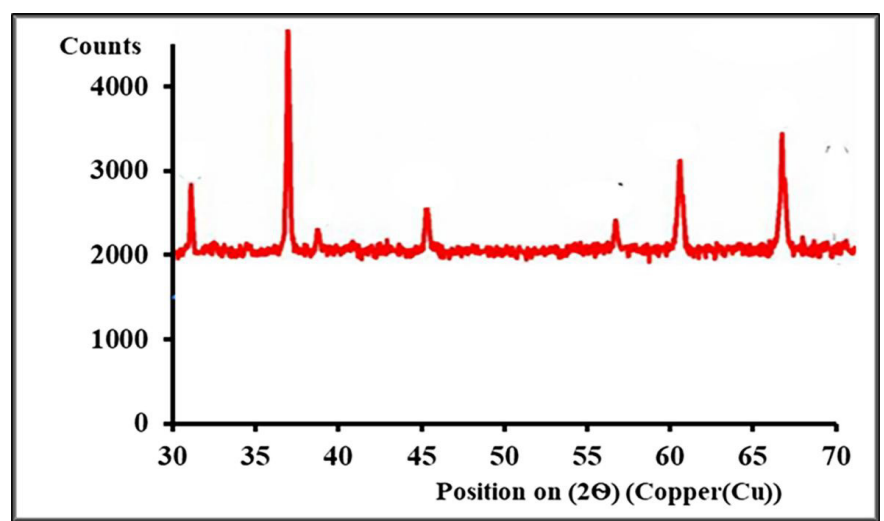


Fig. 7. XRD pattern of green synthesised cobalt oxide nanoparticles.

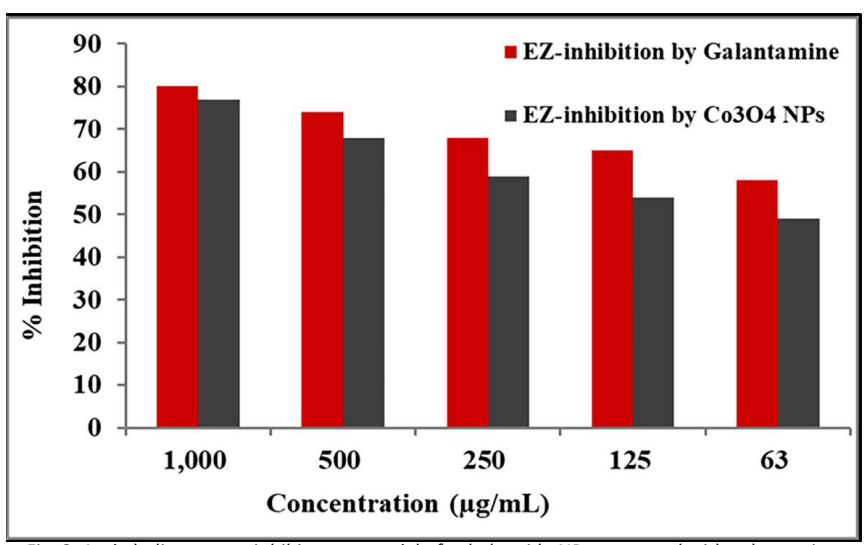


Fig. 8. Anti-cholinesterase inhibitory potential of cobalt oxide NPs compared with galantamine.

produced through the binning of Co3O4- NPs to the active sites of enzymes, blocking substrate binding and reducing enzyme activity. on the other hand , Interaction with Co3O4 NPs may be induced conformational changes in enzymes, affecting their activity.

Our findings are in line with previous study for *Erythrophleum guineense* plant extract as a reducing agent (Zainab et al. 2022) [29], but with improved inhibition efficacy at the same concentrations.

# Beta-hematin (BH) inhibitor Inhibitor of beta-hematin (BH)

In vitro research employed a colorimetric method to verify that Co₃O₄-NPs can inhibit heme crystallization, confirming the hypothesis proposed by Chinappi et al. [30]. The colorimetric

method yielded substantial evidence, highlighting the development rate of heme crystals and revealing considerable variations in BH generation with and without the presence of commercial chloroquine (CQ) and  $Co_3O_4$ -NPs. To use  $Co_3O_4$ -NPs as a heme crystallization inhibitor in comparison with commercial CQ, we examined the influence of time on the rate of BH formation (Fig. 9).

Every 30 seconds, the absorbance of each sample at 400 and 700 nm was measured using a double-beam spectrophotometer. The optimal incubation duration, determined by the start of crystallization and the development rate of heme crystals in each sample, has been examined. (Fig. 9) illustrates that the most substantial reduction of BH production occurred when  $\text{Co}_3\text{O}_4\text{-NPs}$  were utilized as an inhibitor, in contrast to commercial CQ.

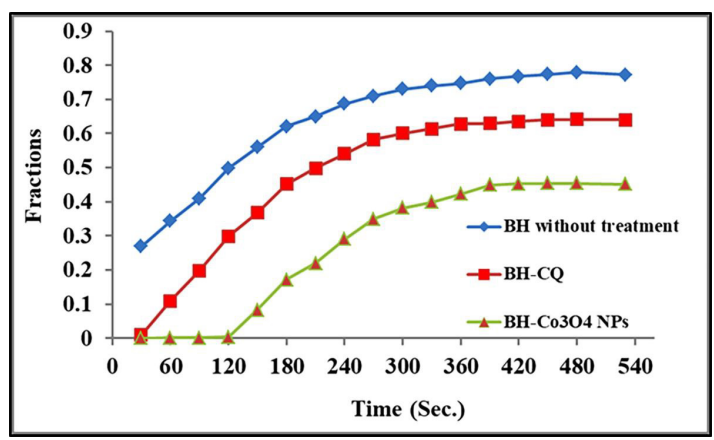


Fig. 9. Time affects BH formation after adding CQ and  $Co_3O_4$ -NPs.

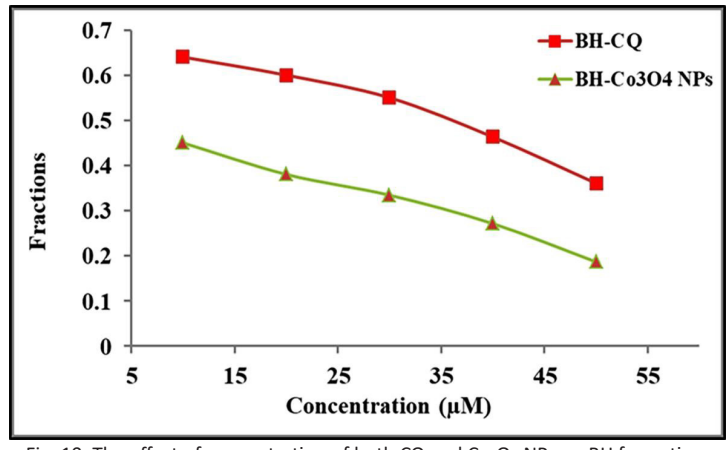


Fig. 10. The effect of concentration of both CQ and  ${\rm Co_3O_4}$ -NPs on BH formation.

To identify the distinction between CQ and synthetic CO<sub>3</sub>O<sub>4</sub>-NPs as inhibitors of BH production, various quantities were individually examined following each addition to hemin chloride, and the growth rate of BH was assessed via spectrophotometry. Generally, results revealed that CO<sub>3</sub>O<sub>4</sub>-NPs inhibited BH formation more effectively than commercial CQ especially at the highest concentration as presented in (Fig. 10), this may be due to their binding to heme, preventing its crystallization into BH or due to their surface properties which influences heme binding and inhibition. These results are approximately similar to previous findings by (Rana et al. 2024) [4].

#### CONCLUSION

This work presents effective green synthesis of cobalt oxide nanoparticles (Co<sub>2</sub>O<sub>4</sub>-NPs) with leaf extract from Rosmarinus Officinalis L. (rosemary). The produced nanoparticles demonstrated strong enzyme and BH inhibitors. The green synthesis method emphasizes the benefits of plant-mediated nanoparticle synthesis, in which a sustainable and green strategy can be followed. These findings provide opportunities for biological applications, notably in disease states when it would be perfect to have antimalarial effect or inhibition of enzymes. Additionally, promising AChE inhibitory characteristics of our generated samples cobalt oxide nanoparticles provide the possibility of therapeutically treating neurodegenerative illnesses, including Alzheimer. While the results are promising, further studies are necessary to explore the mechanisms of action and potential toxicity of these nanoparticles for clinical applications.

#### **ACKNOWLEDGEMENTS**

This research was funded by authors, those who would like to thank the Chemistry Departments of the University of Babylon and Basrah, for providing laboratory equipment.

# **CONFLICT OF INTEREST**

The authors declare that there is no conflict of interests regarding the publication of this manuscript.

#### **REFERENCES**

 Sarah Mohanad Y, Asmaa AH, Ruqaya MA-E. Antibacterial Activity of Silver Nanoparticles Using Salvia officinalis Extract on Some Pathogenic Bacteria. Journal of Pharmacy and Pharmacology. 2019;7(5).

- Bidan AK, Al-Ali ZSA. Oleic and Palmitic Acids with Bioderivatives Essential Oils Synthesized of Spherical Gold Nanoparticles and Its Anti-Human Breast Carcinoma MCF-7 In Vitro Examination. BioNanoScience. 2023;13(4):2293-2306.
- Bidan AK, Al-Ali ZSA. Assessment Defeating of Breast Cancer MCF-7 Cells, and Bacterial Species by Spherical Gold Nanoparticles Fabricated Through Reductive Ability of Framed Bio-Organic Molecules. Chemistry Africa. 2024;7(7):3789-3808.
- Al-Refaia RAA-AK, Alrikabi E, Alkarimi AA, Vasiliadou R. A New Synthesis of Copper Nanoparticles and Its Application as a Beta-Hematin Inhibitor. Indonesian Journal of Chemistry. 2024;24(1):152.
- Arun Paul C, Ranjith Kumar E, Abd El-Rehim AF, Yang G. Cobalt oxide nanoparticles for biological applications: Synthesis and physicochemical characteristics for different natural fuels. Ceram Int. 2023;49(24):40244-40257.
- Junejo B, Solangi QA, Thani ASB, Palabiyik IM, Ghumro T, Bano N, et al. Physical properties and pharmacological applications of Co<sub>3</sub>O<sub>4</sub>, CuO, NiO and ZnO nanoparticles. World J Microbiol Biotechnol. 2023;39(8).
- Paulsson-Habegger L, Snabaitis AK, Wren SP. Enzyme inhibition as a potential therapeutic strategy to treat COVID-19 infection. Bioorganic and Medicinal Chemistry. 2021;48:116389.
- 8. Iravani S, Varma RS. Sustainable synthesis of cobalt and cobalt oxide nanoparticles and their catalytic and biomedical applications. Green Chem. 2020;22(9):2643-2661.
- Emerging Trends in Nanotechnology. Springer Singapore; 2021
- Lugun O, Singh J, Thakur RS, Pandey AK. Cobalt oxide (Co3O4) nanoparticles induced genotoxicity in Chinese hamster lung fibroblast (V79) cells through modulation of reactive oxygen species. Mutagenesis. 2022;37(1):44-59.
- Arif M, Ullah R, Ahmad M, Ali A, Ullah Z, Ali M, et al. Green Synthesis of Silver Nanoparticles Using Euphorbia wallichii Leaf Extract: Its Antibacterial Action against Citrus Canker Causal Agent and Antioxidant Potential. Molecules. 2022;27(11):3525.
- Bidan AK, Al-Ali ZSA. The role of biomaterial constituents of Jasminum sambac (L.) Aiton leaves in copper nanoparticles synthesis and evaluates their activities as anti-breast cancer and antibacterial agents. Inorganic and Nano-Metal Chemistry. 2024;55(6):641-656.
- Dimitrova DZ, Balabanova V. Antioxidant and acetylcholinesterase inhibitory potential of Arnica montana cultivated in Bulgaria. Turkish Journal of Biology. 2012.
- Ferreira J, Santos S, Pereira H. In Vitro Screening for Acetylcholinesterase Inhibition and Antioxidant Activity of Quercus suber Cork and Corkback Extracts. Evid Based Complement Alternat Med. 2020;2020(1).
- 15. Howes LG. Cardiovascular Effects of Drugs Used to Treat Alzheimer's Disease. Drug Saf. 2014;37(6):391-395.
- Hampel H, Mesulam MM, Cuello AC, Farlow MR, Giacobini E, Grossberg GT, et al. The cholinergic system in the pathophysiology and treatment of Alzheimer's disease. Brain. 2018;141(7):1917-1933.
- Guo AJY, Xie HQ, Choi RCY, Zheng KYZ, Bi CWC, Xu SL, et al. Galangin, a flavonol derived from Rhizoma Alpiniae Officinarum, inhibits acetylcholinesterase activity in vitro. Chemico-Biological Interactions. 2010;187(1-3):246-248.
- Al-Refai'a RAK. Cowpea mosaic virus (CPMV) as a carrier vehicle for antimalarial drugs, modification and application. International Journal of Drug Delivery Technology.

J Nanostruct 15(4): 2100-2111, Autumn 2025



- 2019;9(o3).
- 19. Rahman K, Khan SU, Fahad S, Chang MX, Abbas A, Khan WU, et al. Nano-biotechnology: a new approach to treat and prevent malaria. International Journal of Nanomedicine. 2019;Volume 14:1401-1410.
- 20. Veeragoni D, Deshpande SS, Singh V, Misra S, Mutheneni SR. In vitro and in vivo antimalarial activity of green synthesized silver nanoparticles using Sargassum tenerrimum a marine seaweed. Acta Trop. 2023;245:106982.
- López YC, Antuch M. Morphology control in the plantmediated synthesis of magnetite nanoparticles. Current Opinion in Green and Sustainable Chemistry. 2020;24:32-37.
- Chelliah P, Wabaidur SM, Sharma HP, Jweeg MJ, Majdi HS, Al. Kubaisy MMR, et al. Green Synthesis and Characterizations of Cobalt Oxide Nanoparticles and Their Coherent Photocatalytic and Antibacterial Investigations. Water. 2023;15(5):910.
- Zainab, Ahmad S, Khan I, Saeed K, Ahmad H, Alam A, et al. A study on green synthesis, characterization of chromium oxide nanoparticles and their enzyme inhibitory potential. Front Pharmacol. 2022:13.
- 24. Al-Refaia RAK, Alkarimi AA. Synthesis and Hemozoin Inhibitor of Side-Chain Modified Copper-Chloroquine Derivatives. IOP Conference Series: Materials Science and Engineering.

- 2020;987(1):012021.
- 25. El Bachiri A, Soussi L, Karzazi O, Louardi A, Rmili A, Erguig H, et al. Electrochromic and photoluminescence properties of cobalt oxide thin films prepared by spray pyrolysis. Spectrosc Lett. 2019;52(1):66-73.
- 26. Jadhav CH, Pisal KB, Chavan AR, Patil SM, Patil PB, Pagare PK. Electrochemical supercapacitive performance study of spray pyrolyzed cobalt oxide film. Materials Today: Proceedings. 2021;43:2742-2746.
- Singh B, Day CM, Abdella S, Garg S. Alzheimer's disease current therapies, novel drug delivery systems and future directions for better disease management. Journal of Controlled Release. 2024;367:402-424.
- 28. Walczak-Nowicka ŁJ, Herbet M. Acetylcholinesterase Inhibitors in the Treatment of Neurodegenerative Diseases and the Role of Acetylcholinesterase in their Pathogenesis. Int J Mol Sci. 2021;22(17):9290.
- Zainab, Saeed K, Ammara, Ahmad S, Ahmad H, Ullah F, et al. Green Synthesis, Characterization and Cholinesterase Inhibitory Potential of Gold Nanoparticles. Journal of the Mexican Chemical Society. 2021;65(3).
- 30. Chinappi M, Via A, Marcatili P, Tramontano A. On the Mechanism of Chloroquine Resistance in Plasmodium falciparum. PLoS One. 2010;5(11):e14064.

J Nanostruct 15(4): 2100-2111, Autumn 2025